MATERIALE PLASTICE
https://revmaterialeplastice.ro
https://doi.org/10.37358/Mat.Plast.1964

The Influence of Hybrid Matrices Based on Dammar on the Mechanical Properties of Composites with Chopped Corn Cobs Reinforcement

DUMITRU BOLCU[1], MARIUS MARINEL STANESCU[1*], COSMIN MIHAI MIRITOIU[1*], ION CIUCA[2], ALEXANDRU BOLCU[1], IOAN ALEXANDRU RADOI[1]
[1] University of Craiova, Faculty of Mechanics, 107 Calea Bucuresti, 200512, Craiova, Romania
[2] Politehnica University of Bucharest, Faculty of Engineering and Materials Science, 313 Splaiul Independenței, 060042, Bucharest, Romania

Abstract*. As the amount of agricultural waste produced annually worldwide is very high, numerous studies have been conducted with the aim of using them in the structure of composite materials that have a minimal impact on the environment, reduced costs, and can be used in various fields of activity. In this research, four types of composite materials were cast, with a reinforcement of chopped corn cobs and with a matrix of acrylic resin, respectively, of three hybrid resins having various mass proportions, where Dammar natural resin prevailed. The chemical structure of the composites with hybrid matrix was determined using molecular spectroscopic microanalysis, and some mechanical properties of all the composites were investigated. It was found that the values of the obtained mechanical characteristics were limited.*

Keywords*: Hybrid resin, chopped corn cobs, composite materials, FTIR and Raman analyses, mechanical properties*

1. Introduction

Hybrid resins are biopolymers obtained by combining an organic constituent with an inorganic one and are primarily used in the coatings industry [1, 2]. An example of an organic constituent that has been studied in recent years is Dammar resin, which is obtained from the Dipterocarpaceae tree family in East Asia and is used for making wood varnishes or varnishes for paintings [3].

Some properties of composite materials with hybrid resins based on Dammar and natural reinforcements have been studied in [4, 5].

Due to their abundance in nature and the short cycles in which they are produced, research in the last decade has focused on the development of composite materials using matrices made of natural/hybrid resins and reinforcements from agricultural waste. Examples of such waste include cereal straws, seed shells, corncobs, and corn stalks, among others. For instance, corn cobs (without grains) are obtained after corn production and represent a rich biomass resource [6, 7]. Approximately 18 kg of corn cobs are obtained for every 100 kg of corn grains produced [8], and globally, about 164 million tons are produced annually [9, 10]. They are characterized by limited mechanical strength. The structural fiber components of corn cobs are the same as those in wood sawdust (see, for example, [11, 12]), and the cost per ton of corn cobs is approximately 50% lower than the cost of an equivalent amount of wood sawdust, depending on the type of wood, or the corn variety [13, 14].

A parametric study on the thermal insulation of constructions using agglomerated panels made of corn cob granules and wood glue was conducted in [15]. Specifically, this study examined the impact of the thickness of these panels on their thermal insulation performance.

In the work [16], compression tests were conducted on composite materials reinforced with particles from corn cobs and a lignosulfonate matrix. The influence of particle content, the size of the particles and the compaction pressure applied to the composite on compressive strength during processing were also investigated. It was found that with an increase in compaction pressure and particle content, there

**email: mamas1967@gmail.com; miritoiucosmin@yahoo.com*

is an increase in compressive strength. Additionally, the size and shape of the particles were identified as the most influential parameters on mechanical properties.

The mechanical properties of composites with an epoxy resin matrix and reinforcement from corn cob particles and fiberglass flakes were investigated in [17]. An optimal ratio of quantities among the three components (resin, particles, and flakes) was studied to achieve the highest values of tensile, bending, and impact strength.

In [18], the mechanical properties of composites with reinforcement from corn cob splinters with a limited mass ratio and a matrix of a PLA (Polylactic Acid) bio-resin were investigated. The purpose of creating such composites was to replace a small part of pure PLA with chopped corn cobs, thereby reducing the final costs of the composites and their carbon footprint.

In this article, composite materials were fabricated with a hybrid matrix (based on Dammar natural resin and acrylic resin) and reinforcement made of chopped corn cobs (without grains). The behavior of these composites under various types of mechanical stress was studied, including tensile stress, compression and vibrations. Their chemical structure was determined based on Raman and FTIR analyses, and the breaking surface was investigated through SEM analysis.

2. Materials and methods

2.1. Manufacture of samples

The matrix used for casting the composite materials was an acrylic resin of the Claro Cit type and the corresponding hardener, hereafter abbreviated as A. Additionally, three hybrid resins were obtained by combining varying mass percentages of 60, 65, and 70% Dammar natural resin with 40, 35, and 30% Claro Cit resin and the corresponding hardener (the synthetic component was used to initiate polymerization). The hybrid resins will be abbreviated as B, C, and D.

Some mechanical characteristics of the acrylic resin were studied in [19], and the mechanical properties of the hybrid resins were determined in [20, 21].

Corn cobs (without grains) were ground using a hammer mill. The mill screen was adjusted to achieve a particle size of 3 – 5 mm for the chopped cobs.

Four composite material plates of the same thickness were cast, each with a matrix of one of the four types of resins and reinforcement from chopped corn cobs. To ensure proper impregnation of the reinforcement with the matrix, a mass percentage of 40% chopped corn cobs was used for each plate (if the mass percentage exceeded 40%, it was observed that some of the reinforcement did not have enough resin to impregnate, resulting in bonding issues between interfaces; if the mass percentage was less than 40%, an excess of resin appeared in the composite structure). From each plate, 15 tensile samples were cut. Using the same four types of composites used for the plates, four sets of 15 compression samples were cast in cylindrical silicon molds.

Since the mechanical properties of the composite materials made with hybrid matrix and chopped corn cob reinforcement were limited, it was challenging to find practical applications for them.

The mechanical tests performed adhered to the requirements, specifications, and characteristics specified in the corresponding standards: tensile – ASTM D3039/D3039M, compression – ASTM D695.

A uniform pressure of 27 kN/m^2 was applied to the composite material plates and the cylindrical composite samples.

All composite materials were cast at an ambient temperature of 21-23°C. To ensure complete polymerization, samples with an acrylic resin matrix were cut after 5 days of casting, and samples with hybrid resin matrices were cut after 10 days of casting.

The mass proportions of resins, types of fabrics used for face sheets (and their specific mass), dimensions of samples, their abbreviations, and the applied loads are provided in Table 1.

Table 1. Types of resins used, types of fabrics used for face sheets, dimensions of samples, applied loads, and their abbreviations

No.	Type of resin used	Dammar proportion (%)	Sample dimension (mm)	Applied load	Abbr.
1	A	0	250 x 25 x 8 Φ 30 x 60 250 x 25 x 8	tensile compression vibrations	TA CA VA
2	B	60	250 x 25 x 8 Φ 30 x 60 250 x 25 x 8	tensile compression vibrations	TB CB VB
3	C	65	250 x 25 x 8 Φ 30 x 60 250 x 25 x 8	tensile compression vibrations	TC CC VC
4	D	70	250 x 25 x 8 Φ 30 x 60 250 x 25 x 8	tensile compression vibrations	TD CD VD

2.2. Equipment used for testing

The ATR-FTIR spectra for all the composite materials samples made of Dammar based hybrid matrix were recorded by using a Bruker Alpha spectrometer [22] and the Raman spectra were recorded at room temperature by using an inVia confocal Raman microscope (Reinshaw) with a 785 mm laser source and a Peltier cooled CCD detector [23, 24]. The single beam power of the laser was 150 mW and the 50x objective of the microscope was used.

The tensile test was conducted using a Walter+Bai LFM-L Series universal testing machine for static and dynamic tests, with a 25 kN load cell [24], while compression was performed using an LBG Testing Equipment universal testing machine with a 100 kN load cell at a speed of ν = 10mm/min.

The scanning electrone microscopy [25] was performed by using a Phenom Pure Pro X electron microscope, with the maximum magnification of 30000x and an incorporated spectrometer [25, 26].

For the vibration analysis, a data acquisition system SPIDER 8 was used, connected to a signal conditioner type NEXUS 2692-A-0I4, and a notebook for recording experimental data. The connection between the notebook and SPIDER 8 was established using Catman Easy software. An accelerometer from B&K with a sensitivity of 0.04 pC/ms^{-2} was also connected to the signal conditioner. The vibration behavior of samples from sets VA, VB, VC, and VD was investigated as follows: the samples were clamped at one end and left free at the other end; an accelerometer was mounted 5 mm from the free end's edge to record the vibrations; the free length of the samples varied between 100 and 180 mm.

2.3. Theoretical aspects of the characteristic curve shape of composite materials subjected to tension or compression

Since composite materials fall into the category of materials that behave according to Hooke's law, the following relation holds for them:

$$\sigma(t) = E \cdot \varepsilon(t), \tag{1}$$

where t is time, σ is normal stress, E is the modulus of elasticity (Young's modulus), and ε is strain.

The relation between strain and transverse strain during tensile/compressive deformation is:

$$\varepsilon_t(t) = \mp\vartheta \cdot \varepsilon(t), \tag{2}$$

where ϑ is the transverse contraction coefficient, and its inverse is the Poisson's ratio $\left(m = \frac{1}{\vartheta}\right)$.

If the initial cross-section of the tested sample is rectangular with dimensions d_1, d_2, or cylindrical with a diameter d_0, then after deformation, the dimensions of the section will be:

$$d_{1f} = d_1\left(1 \mp \vartheta\varepsilon(t)\right), d_{2f} = d_2\left(1 \mp \vartheta\varepsilon(t)\right), \text{ or } d_f = d_0\left(1 \mp \vartheta\varepsilon(t)\right). \tag{3}$$

Consequently, the cross-sectional area after deformation will be (for both types of sections):

$$S(t) = S_0 \cdot \left(1 \mp \vartheta\varepsilon(t)\right)^2. \quad (4)$$

The force F to which the sample is subjected during deformation and the allowable stress σ_a are given by the relations:

$$F(t) = E \cdot \varepsilon(t) \cdot S_0 \cdot \left(1 \mp \vartheta\varepsilon(t)\right)^2; \quad (5)$$

$$\sigma_a(t) = \frac{F}{S_0} = E \cdot \varepsilon(t) \cdot \left(1 \mp \vartheta\varepsilon(t)\right)^2. \quad (6)$$

The second derivative of the allowable stress is given by the relation (which shows the characteristic curve):

$$\sigma_a''(t) = E \cdot \left(\mp 4\vartheta + 6\vartheta^2\varepsilon(t)\right). \quad (7)$$

It is observed that in the case of compression, the value of the second derivative of the allowable stress is always positive, and consequently, the characteristic curve must have a convex shape.

3. Results and discussions

3.1. The ATR-FTIR and Raman spectra for the composite materials samples with hybrid matrix based on Dammar and the reinforcer made of crushed corn cobs

The influence of different mass percentages of Dammar in the hybrid resins used as matrix on the spectral behaviour of the studied composites was analyzed.

As the investigated samples had been prepared starting from the same precursors, they had similar FT-IR and Raman spectra. The characteristic IR bands for the investigated samples and their assignments are given in Table 2.

Table 2. Characteristic IR bands of the investigated samples and their assignments

Sample	Band (cm^{-1})	Assignment
TB	2924	Stretching C-H of CH_2 and CH
	1723	Stretching C=O in cyclic esters
	1441	Deformation C-H of CH_2 and CH_3
	1128	Wagging and twisting C-H
	980	Stretching C-C
	750	Rocking CH_2
TC	2940	Stretching C-H of CH_2 and CH
	1723	Stretching C=O in cyclic esters
	1441	Deformation C-H of CH_2 and CH_3
	1153	Wagging and twisting C-H
	995	Stretching C-C
TD	2940	Stretching C-H of CH_2 and CH
	1729	Stretching C=O in cyclic esters
	1514	Stretching C-C
	995	Stretching C-C

Table 3 shows the proposed vibrational assignments of the Raman modes.

Table 3. Characteristic Raman bands of the investigated samples and their assignments

Sample	Band (cm^{-1})	Assignment
TB	2905	$\nu(CH_3)$ sym
	1911	$\nu(CH_2)$ sym

	1727	ν(C=O)
	1601	ν(C=C)
	1445	ν(C-C)+δ(CH_2)
	1165	ν(C-C)+δ(CCH)
	798	ω(C-O)+ω(C=O)
TC	2924	ν(CH_3) sym
	1896	ν(CH_2) sym
	1712	ν(C=O)
	1628	ν(C=C)
	1460	ν(C-C)+δ(CH_2)
	810	ω(C-O)+ω(C=O)
TD	2907	ν(CH_3) sym
	1628	ν(C=C)
	1460	ν(C-C)+δ(CH_2)
	1321	δ(CH_2)
	532	δ(COC)

The ATR-FTIR and Raman spectra for the investigated samples are shown in 1a and b.

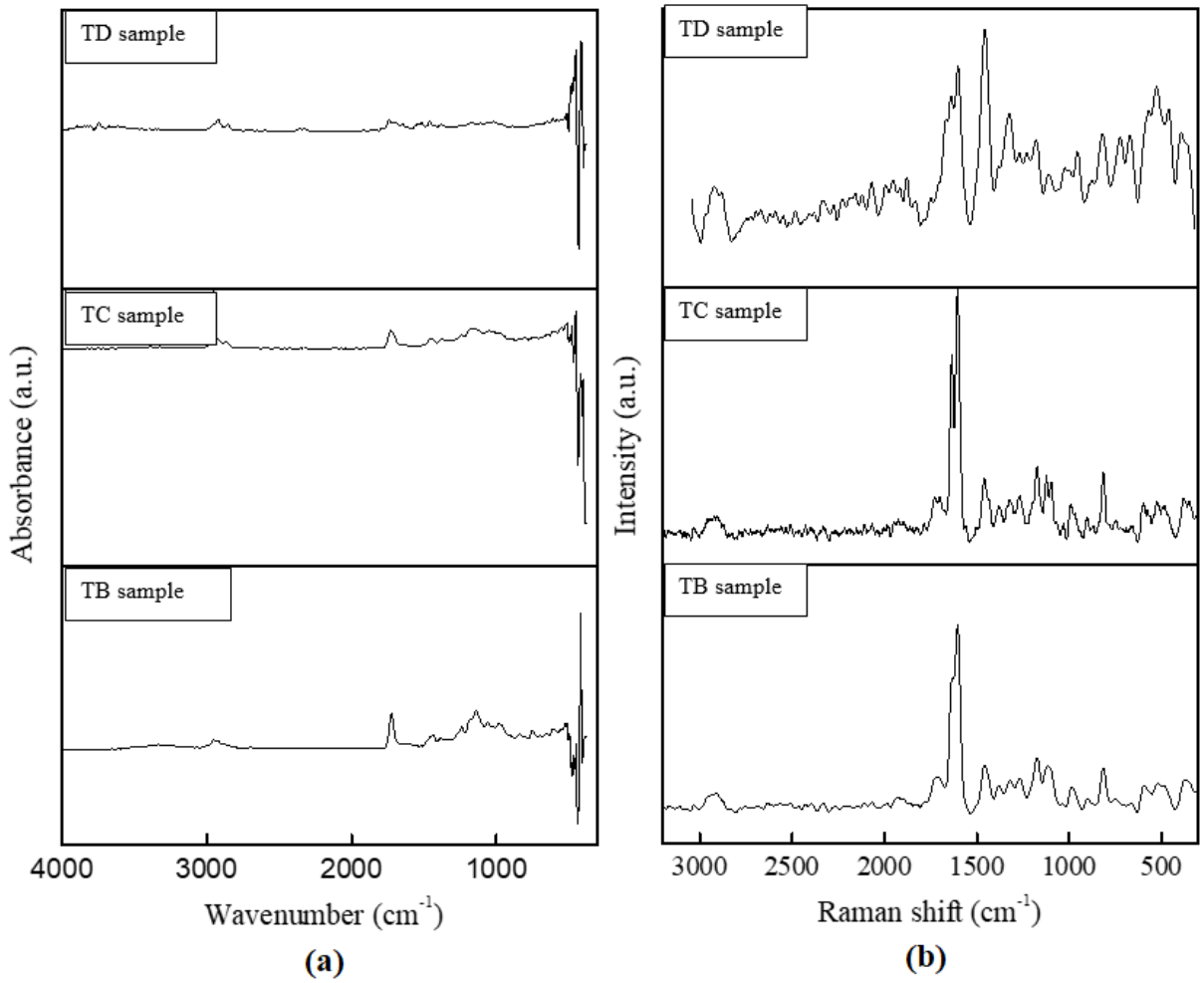

Figure 1. The spectra for the investigated samples: (a) ATR-FTIR; (b) Raman

By analyzing the Table 2, Table 3 and Figure 1 it was found out that the small changes in the samples spectral behaviour reflects the different proportions of acrylic and Dammar resins in their composition. Thus, a decrease in the intensity of their characteristic IR and Raman features with the increase in Dammar content could be evidenced. The quality of the Raman spectrum decreased with the increase in Dammar content.

3.2. Tensile testing of samples TA, TB, TC, and TD

The sets of samples TA, TB, TC, and TD were subjected to tensile testing. Based on this testing, the characteristic curve, tensile strength R_m (MPa), elongation at breaking A (%), and modulus of elasticity E (N/mm^2) were determined for each sample. From each set, a curve was selected and presented in Figure 2, where values close to the arithmetic mean of the mechanical properties were recorded.

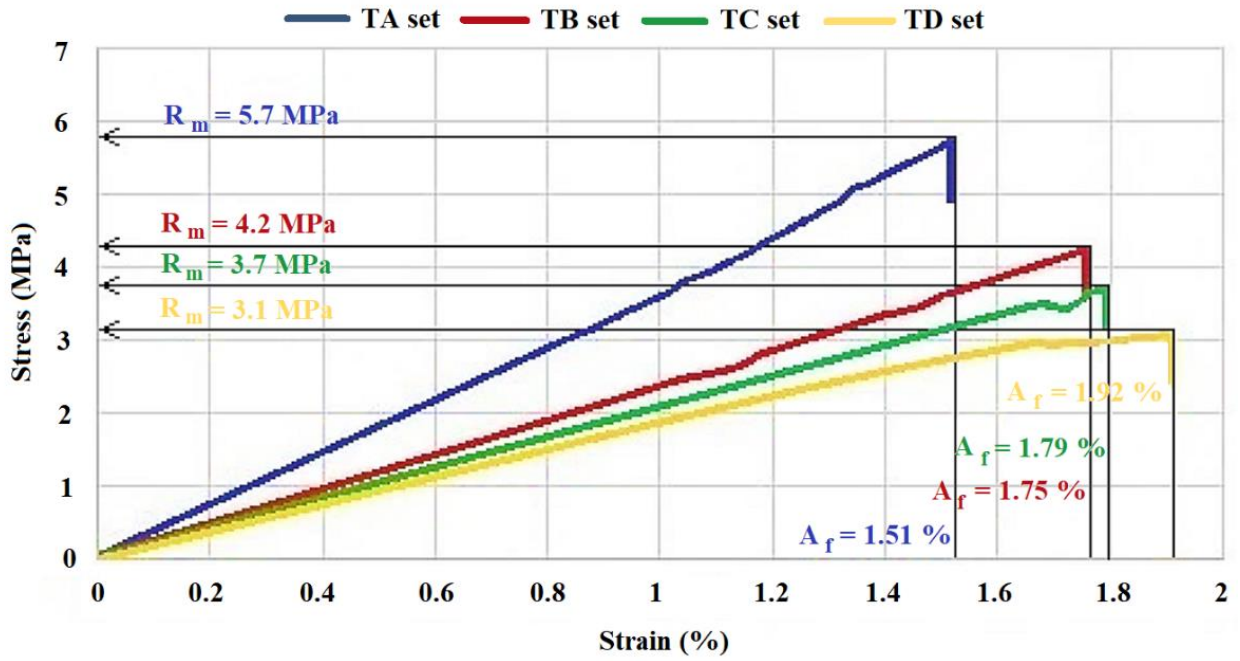

Figure 2. The characteristic curves obtained based on tensile testing, with values close to the arithmetic mean of the mechanical properties for samples from sets TA, TB, TC, and TD

Based on the tensile testing of the sets of samples TA, TB, TC, and TD, Table 4 provides the average value, linear mean deviation, and mean square deviation of the modulus of elasticity E (N/mm^2), tensile strength R_m (MPa), and elongation at breaking A (%).

Table 4. The average value, linear mean deviation, and mean square deviation of the modulus of elasticity, tensile strength, and elongation at breaking obtained based on the tensile testing of sets TA, TB, TC, and TD samples

Sample type	Modulus of elasticity E (N/mm^2)			Tensile strength R_m (MPa)			Elongation at breaking A (%)		
	$\bar{x}$	$\overline{d_x}$	$\overline{\sigma_x}$	$\bar{x}$	$\overline{d_x}$	$\overline{\sigma_x}$	$\bar{x}$	$\overline{d_x}$	$\overline{\sigma_x}$
TA	185.6	1.467	1.776	5.678	0.035	0.048	1.509	0.018	0.026
TB	165.16	0.46	0.56	4.203	0.03	0.041	1.75	0.015	0.019
TC	138.2	0.6	0.7	3.7	0.029	0.036	1.78	0.012	0.016
TD	122	0.213	0.288	3.1	0.03	0.041	1.902	0.027	0.031

The analysis of characteristic curves for samples from sets TA, TB, and TC indicates a linear behaviour. There was a proportionality between stress and strain. The load had been absorbed by both the matrix and the reinforcement until the maximum tensile strength was reached. The breaking of the matrix led to the breaking of the composite, as the tensile strength of acrylic resin and of the two hybrid resins with 60 and 65% Dammar was higher than the tensile strength of chopped corn cobs. The tensile strength of corn cobs is 0.26 - 2.5 MPa [27]. Moreover, the irregular shape of the chopped corn cobs caused the formation of stress concentrators, leading to breaking initiation in the region of the chopped cobs, where cracks propagated. The resin region was rapidly loaded with additional high stresses, leading to final breaking.

The characteristic curve of sample TD consists of two linear regions. The first region, between 0 MPa and 3.0 MPa of tensile strength, indicates that the load was equally shared by both the matrix and the reinforcement. The second region, located at the end of the curve, with a shorter length and a smaller slope than the first region, demonstrates that the mass ratio of 70% Dammar in the hybrid resin reduced the tensile strength of the matrix below that of the reinforcement. Reaching the matrix's ultimate tensile strength temporarily transferred the load to the reinforcement until the final breaking of the composite.

3.3. SEM analysis for the samples breaking section

In the Figure 3, the SEM analysis results are presented regarding the breaking section of the four types of composite materials tensile loaded.

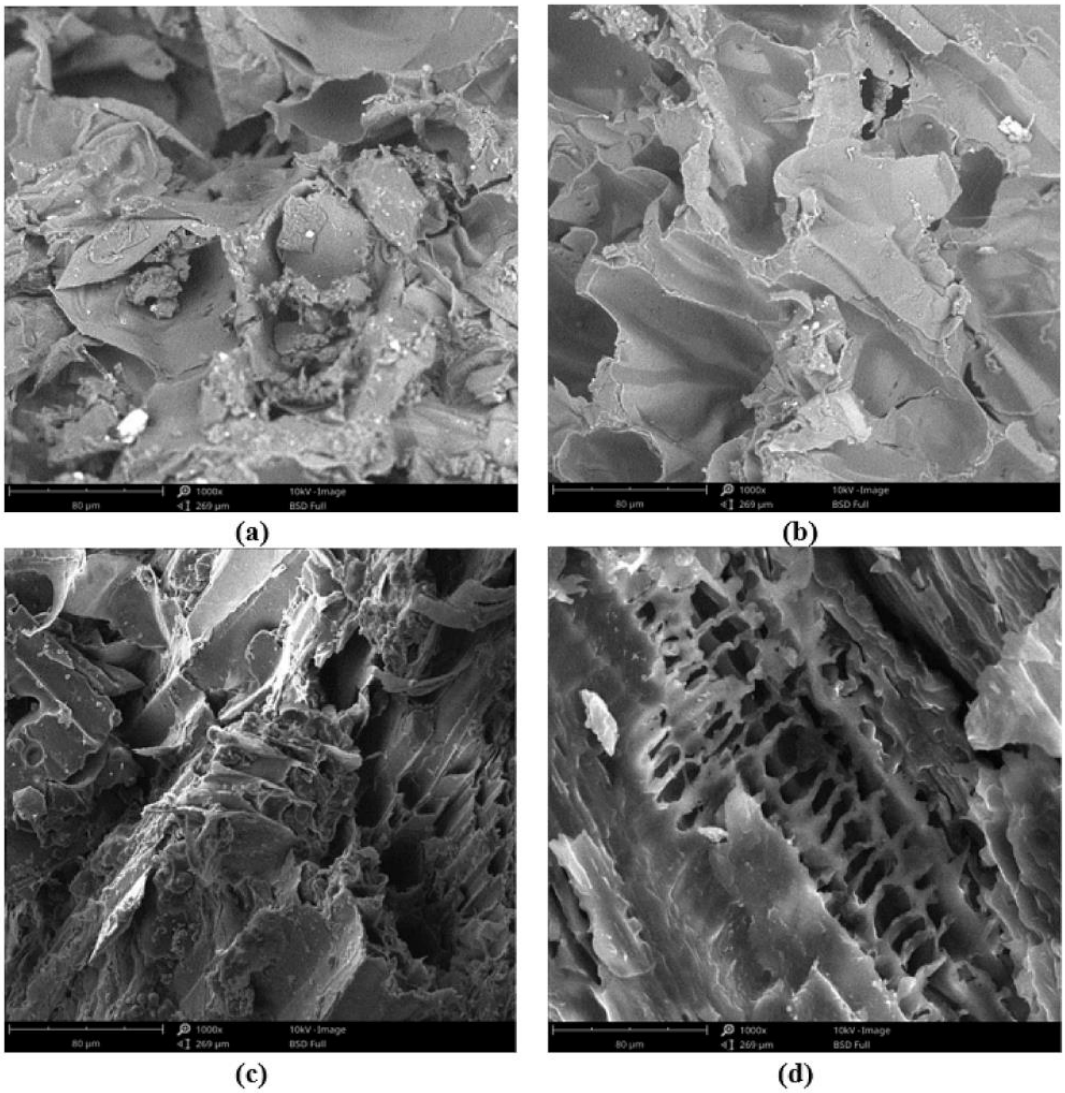

Figure 3. SEM images for the breaking section, related to the samples from the sets: (a) TA; (b) TB; (c) TC; (d) TD

The analysis of the four breaking sections reveals no significant differences between the breaking appearances. Breaking occurred abruptly at the interface between the matrix and the reinforcement, characteristic of brittle materials (breaking without yielding).

The breaking zone in Figure 3a appears smoother than the breaking zones in the other figures. The breaking occurred by the detachment of the pieces of chopped corn cobs from the matrix. A possible

explanation is that the adhesion between the synthetic resin and the natural reinforcement was not very strong.

The breaking zones of samples TB, TC, and TD, presented in Figure 3b - d, are rougher and contain fragments of chopped corn cobs pulled out from the matrix. The cobs were pulled out because the curing time of the hybrid resin was much longer than that of the acrylic resin, allowing chopped cob pieces to impregnate with hybrid resin, aiding in better adhesion between them.

3.4. Compressive testing of samples CA, CB, CC, and CD

The sets of samples CA, CB, CC, and CD were tested under compression. For each sample, the characteristic curve, compressive strength σ_{ac} (MPa), transverse displacement L_{max} (mm), and maximum compressive load F_{max} (kN) were determined. From each set, a curve was selected, and it is presented in Figure 4, where values close to the arithmetic mean of the determined mechanical characteristics were recorded.

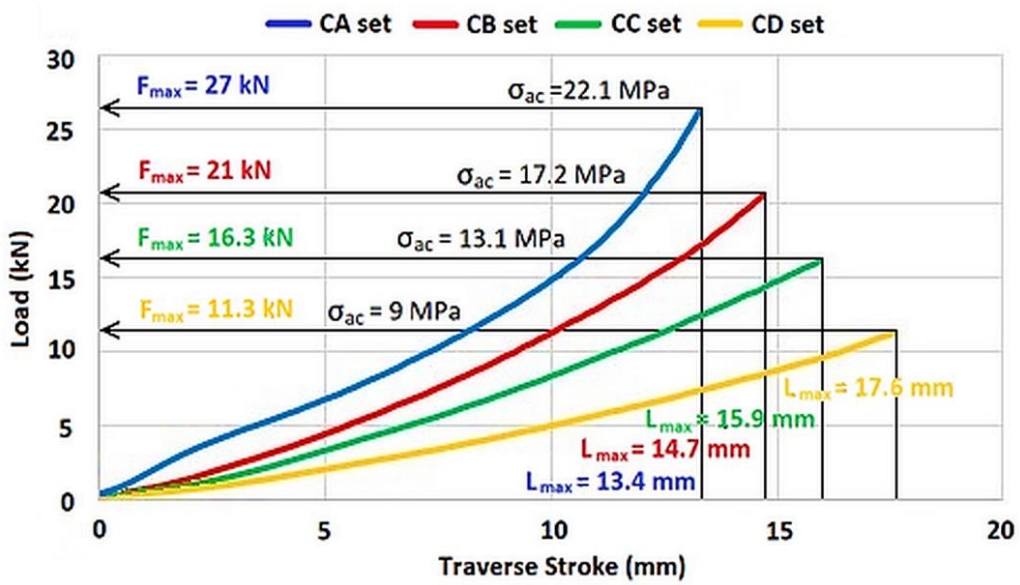

Figure 4. The characteristic curves obtained based on compression testing, with values close to the arithmetic mean of the mechanical properties, for samples from sets CA, CB, CC, and CD

Based on the compression testing of the samples from the CA, CB, CC, and CD sets, Table 5 provides the average value, linear mean deviation, and mean square deviation of compressive strength σ_{ac} (MPa), transverse displacement L_{max} (mm), and maximum compressive load F_{max} (kN).

Table 5. Average value, linear mean deviation, and mean square deviation of compressive strength, transverse displacement, and maximum compressive load for sets CA, CB, CC, and CD

Sample type	Compressive strength σ_{ac}(MPa)			Maximum compressive load F_{max} (kN)			Transverse displacement L_{max} (mm)		
	$\bar{x}$	$\overline{d_x}$	$\overline{\sigma_x}$	$\bar{x}$	$\overline{d_x}$	$\overline{\sigma_x}$	$\bar{x}$	$\overline{d_x}$	$\overline{\sigma_x}$
CA	22	0.253	0.316	26.8	0.317	0.372	13.4	0.173	0.218
CB	17.2	0.151	0.185	21.1	0.212	0.238	14.67	0.129	0.173
CC	13.16	0.124	0.153	16.33	0.098	0.125	16	0.115	0.134
CD	9	0.089	0.118	11.26	0.098	0.13	17.61	0.098	0.126

All the characteristic curves of the composites tested under compression indicate that these materials fall into the category of "tough materials." Specifically, after reaching the elastic limit, material flow was observed, as well as a transverse bulging resembling a barrel shape (a growth of the cross-sectional

area). This allowed the sample to withstand increasing compressive forces until irreversible deformation occurred.

From Figure 4 and Table 5, it is observed that the maximum loading force and compressive strength have decreased with an increasing proportion of Dammar, and in the case of transverse displacement, the process was reversed. For instance, the maximum loading force (and the compressive strength) of sample CA, cast from a composite material with an acrylic resin matrix, was over 25% higher than that of samples CB, over 65% higher than that of samples CC, and over 135% higher than that of samples CD. In the case of the transverse displacement of samples cast from a composite material with an acrylic resin matrix, the maximum loading force and compressive strength showed a decrease of approximately 10% compared to samples CB, approximately 20% compared to samples CC, and approximately 30% compared to samples CD.

3.5. The vibration behaviour of samples VA, VB, VC, and VD

The analysis of free vibrations of the samples provides information regarding certain mechanical characteristics of the studied composite materials.

The damping factor of vibrations and the natural frequency were determined for one sample from each set. Figure 5 illustrates the method of calculating the natural frequency and damping factor for the first natural mode of vibration of a sample from set VA, with values corresponding to a free length of 140 mm.

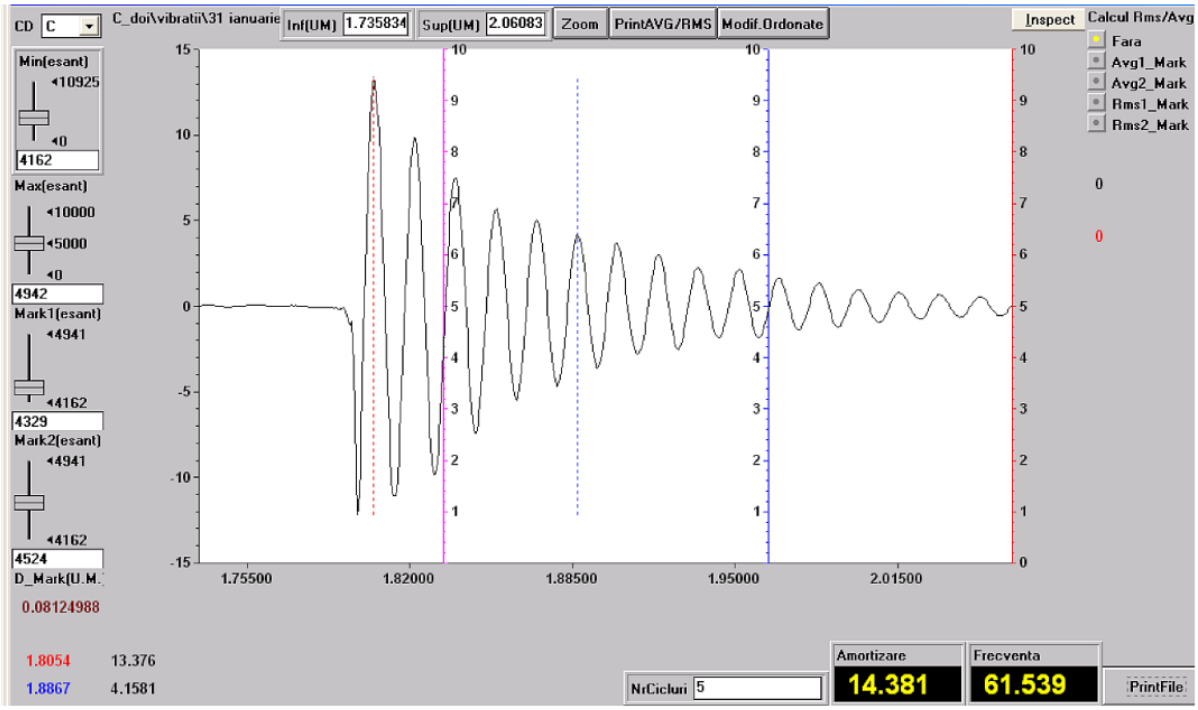

Figure 5. Recording the vibrations for a sample from set VA, with a free length of 140 mm

The damping factor was calculated using the following formula [28, 29]:

$$\mu = \frac{1}{t_2 - t_1} \cdot ln \frac{w_1}{w_2}, \tag{8}$$

where:

- w_1 is the maximum value at the beginning of the measurement interval, and w_2 is the maximum value at the end of the measurement interval, chosen for determining the damping factor;
- t_1 is the time for the maximum w_1 and t_2 is the time for the maximum w_2, from the experimentally recorded diagram used to calculate the damping factor.

Table 6 presents the experimental data obtained for samples from sets VA, VB, VC, and VD.

Table 6. Vibrational behaviour of sample from sets VA, VB, VC, and VD

Free Length (mm)	TA		TB		TC		TD	
	Frequency $\nu(Hz)$	Damping $\mu(s^{-1})$	Frequency $\nu(Hz)$	Damping $\mu(s^{-1})$	Frequency $\nu(Hz)$	Damping $\mu(s^{-1})$	Frequency $\nu(Hz)$	Damping $\mu(s^{-1})$
100	116.6	26.2	81.9	28.4	70	29.7	58.4	30.8
120	80.8	17.6	56	19.1	48.7	20	40.7	21.5
140	61.5	14.4	43.3	15.5	37.3	16.2	31.3	17.2
160	47.1	11	33.2	11.9	28.5	12.4	24	13.2
180	38.2	9.2	27.2	9.9	23.5	10.3	20.2	10.9

The natural frequency and damping coefficient depend on both the boundary conditions and the sample dimensions, as well as the material properties. This multiple dependence of the two characteristics makes them determinable experimentally only. Their behaviour concerning the modulus of elasticity, the mass percentage of Dammar in the hybrid resin, and the vibrating bar length is as follows:

- from the data presented in Table 4 and Table 6, it can be observed that the values of the modulus of elasticity and recorded frequency decreased, while the values of the damping coefficient increased, starting with the samples from set VA, followed by those from set VB, then those from VC and VD;
- the values of natural frequency decreased, and damping factor values increased with the increasing mass percentage of Dammar in the hybrid resin; a possible explanation for this result could be that, with the increasing mass percentage of Dammar, there was an increase in the elasticity of the samples, leading to faster damping of vibrations.

The damping capacity of the materials used in all investigated samples can be appreciated by calculating the loss factor η with the relation [28]:

$$\eta = \frac{\mu}{\pi\nu}. \tag{9}$$

More precisely, for the studied composites, the average loss factor values are:

- $\eta = 0.07328$ for VA composites;
- $\eta = 0.11257$ for VB composites;
- $\eta = 0.13525$ for VC composites;
- $\eta = 0.17155$ for VD composites.

The loss factor values for the studied composite materials indicate that those with a hybrid resin matrix had superior damping properties compared to those with an acrylic resin matrix.

4. Conclusions

Tensile tests of acrylic resin matrix composites (symbolized TA) shown that these materials have:

- lower values of tensile strength and modulus of elasticity and higher values of elongation at break, compared to those of acrylic resin [19];
- the highest values of tensile strength and modulus of elasticity and the lowest elongation at break, compared to TB, TC and TD composites.

Increasing the mass percentage of Dammar in the hybrid resins used as a matrix in the studied composites resulted in:

- decrease in tensile strength and modulus of elasticity;
- increase in ductility, which led to a progressive increase in elongation at breaking;
- decreasing the natural frequency and increasing the damping factor.

The mechanical behaviour of the TB, TC and TD composites kept the evolution trend of the mechanical properties of the hybrid resins used as matrices (whose properties are studied in [20, 21]).

For all studied composite materials, the damping factor was inversely proportional to the square of the bar length. This corresponds to an energy dissipation mechanism where the damping force is proportional to the bending velocity of the bar.

The values of the mechanical properties obtained from the tensile and compression tests of the studied composite materials were limited. Despite this disadvantage, they can be used as core materials for manufacturing sandwich composites that can be used in the construction field or the furniture industry.

References

1.ISHIMURA, T., LU, R., YAMASAKI, K., MIYAKOSHI, T., Development of an eco-friendly hybrid lacquer based on kurome lacquer sap, *Prog. Org. Coat.*, **69**(1), 2010, 12-15. https://doi.org/10.1016/j.porgcoat.2010.04.019
2.KANEHASHI, S., LU, R., OYAGI, H., MIYAKOSHI, T., Developement of bio-based hybrid resin, from natural lacquer, *Prog. Org. Coat.*, **77**(1), 2014, 24-29. https://doi.org/10.1016/j.porgcoat.2013.07.013
3.DIETEMANN, P., HIGGITT, C., KÄLIN, M., EDELMANN, M.J., KROCHENMUSS, R., ZENOBI, R., Aging and yellowing of triterpenoid resin varnishes – Influence of aging conditions and resin composition, *J. Cult. Herit.*, **10**(1), 2009, 30-40. https://doi.org/10.1016/j.culher.2008.04.007
4.BOLCU, D., STĂNESCU, M.M., A study of some mechanical properties of composite materials with a Dammar-based hybrid matrix and two types of flax fabric reinforcement, Polymers, **12**(8), 2020, 1649, https://doi.org/10.3390/polym12081649
5.BOLCU, D., STĂNESCU, M.M., The influence of non-uniformities on the mechanical behaviour of hemp-reinforced composite materials with a Dammar matrix, *Materials*, **12**(8), 2019, 1-15, https://doi.org/10.3390/ma12081232
6.CZAJKOWSKI, Ł., WOJCIESZAK, D., OLEK, W., PRZYBYŁ, J., Thermal properties of fractions of corn stover, *Constr. Build. Mater.*, **210**, 2019, 709-712. https://doi.org/10.1016/j.conbuildmat.2019.03.092
7.MENARDO, S., AIROLDI, G., CACCIATORE, V., BALSARI, P., Potential biogas and methane yield of maize stover fractions and evaluation of some possible stover harvest chains, *Biosyst. Eng.*, **129**, 2015, 352-359. https://doi.org/10.1016/j.biosystemseng.2014.11.010
8.TSAI, W.T., CHANG, C.Y., WANG, S.Y., CHANG, C.F., CHIEN, S.F., SUN, H.F., Cleaner production of carbon adsorbents by utilizing agricultural waste corn cob, *Resour. Conserv. Recycl.*, **32** (1), 2001, 43-53. https://doi.org/10.1016/S0921-3449(00)00093-8
9.TAKADA, M., NIU, R., MINAMI, E., SAKA, S., Characterization of three issue fractions in corn (Zea mays) cob, *Biomass Bioenergy.*, **115**, 2018, 130-135. https://doi.org/10.1016/j.biombioe.2018.04.023
10.ZHOU, Y., FU, J., CHEN, Z., REN, L., The effect of microstructure on mechanical properties of corn cob, *Micron.*, **146**, 2021, 1-7. https://doi.org/10.1016/j.micron.2021.103070
11.BANJO AKINYEMI, A., AFOLAYAN, J.O., OGUNJI OLUWATOBI, E., Some properties of composite corn cob and sawdust particle boards, *Constr. Build. Mater.*, **127**, 2016, 436-441. https://doi.org/10.1016/j.conbuildmat.2016.10.040
12.BHATIA, S.K., JAGTAP, S.S., BEDEKAR, A.A., BHATIA, R.P., PATEL, A.K., PANT, D., BANU, J.R., RAO, C.V., KIM, Y.G., YANG, Y.H., Recent developments in pretreatment technologies on lignocellulosic biomass: Effect of key parameters, technological improvements, and challenges, *Bioresour. Technol.*, 2020, 122724. https://doi.org/10.1016/j.biortech.2019.122724
13.*** CORN-COB, 2023, Corn Cob without kernels https://www.indiamart.com/proddetail/corn-cob-18738834573.html
14.***SAWDUST, 2023, Wood sawdust. https://www.indiamart.com/proddetail/wood-sawdust-2852202179797.htlm

15.PAIVA, A., PEREIRA, S., SÀ, A.B., CRUZ, D., A contribution to the thermal insulation performance characterization of corn cob particleboards, *Energy Build.*, **45**, 2012, 274-279. https://doi.org/10.1016/j.enbuild.2011.11.019
16.TRIBOT, A., DELATTRE, C., BADEL, E., DUSSAP, C.G., MICHAUD, P., De BAYNAST, H., Design of experiments for bio-based composites with lignosulfonates matrix and corn cob fibers, *Ind. Crop. Prod.*, **123**, 2018, 539-545. https://doi.org/10.1016/j.indcrop.2018.07.019
17.GARADIMANI, K.R., RAJU, G.U., KODANCHA, K.G., Study on mechanical properties of corn cob particle and E-glass fiber reinforced hybrid polymer composites, *Am. J. Mater. Sci.*, **5**(3C), 2015, 86-91. https://doi.org/10.5923/c.materials.201502.18
18.De BAYNAST, H., TRIBOT, A., NIEZ, B., AUDONNET, F., BADEL, E., CESAR, G., DUSSAP, C.G., GASTALDI, E., MASSACRIER, L., MICHAUD, P., DELATTRE, C., Effects of Kraft lignin and corn cob agro-residue on the properties of injected-moulded biocomposites, *Ind. Crops Prod.*, **177**, 2022, 1-12, https://doi.org/10.1016/j.indcrop.2021.114421
19.POPA-DIACONU, D., VITALARIU, A., TATARCIUC, M., FRATILA, D., Studies on the mechanical parameters of denture base acrylic resins, *Mater. Plast.*, **57**(4), 2020, 360-365. https://doi.org/10.37358/MP.20.4.5436
20.CIUCĂ, I., STĂNESCU, M.M., BOLCU, D., MIRIȚOIU, C.M., RĂDOI, A.I., Study of mechanical properties for composite materials with hybrid matrix based on dammar and natural reinforcers, *Environ. Eng. Manag. J.*, **21**(2), 2022, 299-307.
21.RĂDOI, A.I., CIUCĂ, I., STĂNESCU, M.M., BOLCU, D., NICOLICESCU, C., MIRIȚOIU, C.M., BOGDAN, M., Studies regarding some mechanical properties for a hybrid resin used to build composites reinforced with corn cob powder, *Mater. Plast.*, **59**(2), 2022, 24-31. https://doi.org/10.37358/MP.22.2.5581
22.***BRUKER, 2023, Bruker Alpha II FTIR Spectrometer Portable Spectral Services. https://www.portaspecs.com/product/ft-ir-atr-eg-powders/
23.***inVia, 2023, confocal Raman microscope. https://www.renishaw.com/en/invia-confocal-raman-microscope--6260
24.***WALTER+BAI, 2023, Walter+Bai Single Column Electromechanical Testing Machines Series LFM-L.https://www.walterbai.com/page/documents/Procuct_Informations/LFM-L_up_to_25_kN_ Product_Information_E.pdf
25.***DESKTOP-SEM, 2023, Electron microscopy, Phenom Desktop SEM, Desktop scanning electron microscopes for high-performance, high-quality imaging and analysis. https://www.thermofisher.com/ro/en/home/electron-microscopy/products/scanning-electron microscopes.html?cid=msd_ms_sbu_xmkt_sem_123456_emea_pso_gaw_8n2ujm&gad_source=1&gclid=EAIaIQobChMIkISM6veJhAMVIYuDBx0TEgkSEAAYAiAAEgKZYPD_BwE
26.***PHENOM, 2023. Phenom Pure. https://total-spectrum.ro/categorii-produse/microscoape-electronice-de-baleiaj-sem-7/produse/phenom-pure-29
27.OLUMOYEWA, D.A., ODEYEMI, S.O., OLUGBENGA, A.L., MODUPE, A.E., Physical and mechanical properties evaluation of corncob and sawdust cement bonded ceiling boards, *Int. J. Eng. Res. Afr.*, **42**, 2019, 65-75. https://doi.org/10.4028/www.scientific.net/JERA.42.65
28.STĂNESCU, M.M., BOLCU, D., PASTRAMĂ, S.D., CIUCĂ, I., MANEA, I., BACIU, F., Determination of damping factor at the vibrations of composite bars reinforced with carbon and kevlar texture, *Mater. Plast.*, **47**(4), 2010, 492-496.
29.BURADA, C.O., MIRIȚOIU, C.M., BOLCU, D., STĂNESCU, M.M., Experimental determinations of the damping factor and stiffness for new sandwich platbands with different reinforcement and core, *Rev. Rom. Mater.*, **44**(4), 2014, 405-413.

Manuscript received: 28.06.2024